Composite Structures 97 (2013) 189–201

Contents lists available at SciVerse ScienceDirect

Composite Structures

journal homepage: www.elsevier.com/locate/compstruct

Numerical simulation of the Lamb wave propagation in honeycomb sandwich panels: A parametric study

Seyed Mohammad Hossein Hosseini *, Ulrich Gabbert

Institute of Mechanics, Department of Mechanical Engineering, Otto-von-Guericke-University Magdeburg, Universitätsplatz 2, 39016 Magdeburg, Germany

ARTICLE INFO

Article history:
Available online 7 November 2012

Keywords:
Lame wave propagation
Honeycomb sandwich plate
Parametric study
Homogenization
Finite element method

ABSTRACT

The paper aims to describe the guided Lamb wave propagation in honeycomb sandwich panels. The application of Lamb waves is a well-known method in modern online structural health monitoring techniques. To analyze the wave propagation in such a complicated geometry with an analytical solution is hardly possible; therefore a dimensional finite element simulation is used. A piezoelectric actuator is used to excite the waves on the sandwich panel surface. The extended model of the honeycomb sandwich panel is consisting of two plate layers and a mid-core layer. In addition, a simplified model is used to reduce the computing costs, where the mid-core of the sandwich panel is replaced by a homogeneous layer. The results from the extended model and the simplified model are in most cases in a good agreement; however the limitations of using the simplified model are discussed. A parametric study is used to show the influence of the geometrical properties of honeycomb plates, the material properties of the skin plates and the loading frequency on the group velocity, the wave length and the energy transmission. Each of these properties provides valuable information to design an efficient health monitoring system. Finally, an experimental test is presented.

1. Introduction

Using Lamb waves generated and received by a mesh of piezoelectric (PZT) actuators and sensors is a developing technology for structural health monitoring (SHM) in composite structures [1,2]. Due to the high sensitivity, the possibility of an online monitoring and the low cost of the required equipments, make Lamb waves based damage detection an interesting SHM technique for many industries [1].

For the first time the brothers Jacques and Pierre Curie found the PZT effect in a single crystal such as the Rochelle salt. Nowadays, PZT elements can be found in different shapes, for instance, as films, plates, powders, stacks and etc. The application of PZT elements for SHM applications has to take into account several aspects, such as, a minimal influence on the plate strength and a good bonding to the plate in the working temperature range [3]. The PZT effect can be expressed as an interaction between the electrical and mechanical energy. By applying an electrical field, dimensional changes will occur in the material. Conversely, by applying mechanical deformations, a voltage corresponding to the strain will come out of the PZT element [4].

The sensitivity of the Lamb waves to small damages [3] results in reliable advantages in terms of the location, the severity and the type of the damages. Lamb waves are categorized as elastic waves that can propagate in a solid plate with free surfaces. Horace Lamb was the first who described Lamb waves mathematically. However, Lamb waves were used for nondestructive materials testing for two decades [5], but still the wave propagation in heterogeneous plates, such as honeycomb structures is at research level [1,3].

A new method of non-destructive testing of honeycomb plates was introduced by Thwaites and Clark [6]. Within this method localized phase velocities in reverberant panels in the frequency range of 5–50 kHz was measured. The ability of the method was proved to detect delamination and core crazing in honeycomb sandwich panels unambiguously. In another study by Wierzbicki and Woźniak a homogenization technique based on a dispersive model of periodic composite solids made of an isotropic matrix reinforced by a honeycomb-like slender skeleton was formulated for the analysis of vibration and wave propagation problems [7]. It was proved that the proposed method has the advantage to describe the effect of cell size on the overall dynamic behavior of a composite solid. An isotropic response of honeycomb based composites has been reported on the macro-level.

A two-dimensional finite element model of the unit cell and the application of the theory of periodic structures was used in [8] by Ruzzene et al. to investigate the effect of the geometry of unit cells on the dynamics of the propagation of elastic waves within the

* Corresponding author.
E-mail addresses: rsg.931@gmail.com (S.M.H. Hosseini), Ulrich.Gabbert@ovgu.de (U. Gabbert).

0263-8223/$ - see front matter © 2012 Elsevier Ltd. All rights reserved.
http://dx.doi.org/10.1016/j.compstruct.2012.09.055

cellular structure. The ability of the method was shown to achieve the desired transmissibility levels in specified directions for optimal design configurations to obtain efficient vibration isolation capabilities. In addition, in a study by Mustapha et al. the fundamental anti-symmetric Lamb mode (A_0) was loaded at a low frequency used to detect debonding in sandwich CF/EP composite structures with a honeycomb core. Within this study the experimental results were compared with results obtained from finite element analysis. In the finite element analysis the core layer was homogenized as an orthotropic material and modeled with eight-node 3-D brick elements. The location of the damage was detected using the time of the flight of damage-reflected waves. It has been reported that the experimental results correspond very well with results which were obtained with this simplified finite element model [9]. A similar study by Xue et al. was done, in which ultrasonic guided waves were used to detect the delamination between skin and honeycomb of a composite helicopter rotor blade. They used a theoretical approach based on the global matrix method. In addition, finite elements and experimental studies were also taken into account. In numerical and theoretical approaches the honeycomb core layer was also replaced by a homogenized layer. Corresponding results from different methods have been reported in [10].

A dimensional finite element was used by Song et al. [1], to study the Lamb wave propagation in honeycomb sandwich panels. The results were compared with a simplified model where the core layer was replaced by a heterogeneous material with a simple cubic geometry. It has been reported that the agreement of the results calculated with the extended honeycomb model in comparison to the simplified model depends on the frequency of the loading signal. The results were validated by experimental results.

In the present paper the dependency of the wave propagation on different geometrical properties of honeycomb sandwich panels, such as, honeycomb core size, cover plate thickness, thickness of the honeycomb core size is studied. The Lamb waves are examined on the top and the bottom surfaces of the structure. In addition, a simplified model where the complicated honeycomb midcore of the sandwich panel is replaced by a simple homogeneous layer with orthotropic mechanical properties is considered. Fig. 1 shows a schematic representation of different models which are investigated, including the honeycomb sandwich panel and the simplified model. This parametric study provides fundamental knowledge of Lamb wave behavior in honeycomb sandwich panels which is essential to design efficient SHM systems [11]. These information are needed for choosing the appropriate loading signal for SHM applications [9] as well as the determination of possible damages which can be detected by the propagating wave in the signal processing level [3].

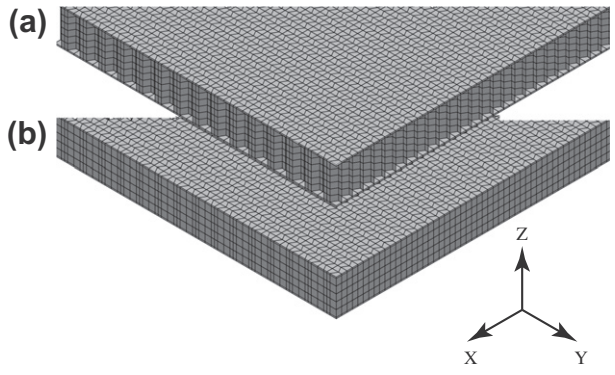

Fig. 1. Schematic representation of different models: (a) honeycomb sandwich panel and (b) simplified model.

2. Finite element modeling

A honeycomb sandwich panel consists of two skin plates and a honeycomb core layer. Fig. 2 shows the description of geometrical dimensions of the panel. Within our study the influences of the cover plate thickness (t_p), the honeycomb wall thickness (t_h) and the honeycomb core size (H_c) on the wave propagation are evaluated. However, the honeycomb height, the PZT element sizes, the length and the width of the plate will remain constant, cf. Table 1. The material properties of the honeycomb sandwich panel components are provided in Table 2.

The skin plates are modeled using 3-D solid elements. 2-D shell elements are used to model the honeycomb cells. The transition region, where the solids connect to the shells, is often the weakest area and an accurate modeling approach is needed to consider the correct stresses and deformation. In applications where only small deformation occurs, such as wave propagation in a plate, multi-point constraint equations are a reliable method to connect two portions of a structure using solids and shells [12]. In the present study an automatic constraint equation developed by ANSYS® between elements is used to connect the shell and the solid elements. Finally, 3-D electromechanical coupled solid elements are used to model the actuators and sensors [1].

In addition, the wave propagation in a simplified model is studied. In this case, the core layer is modeled with 3-D solid elements with orthotropic material properties. The orthotropic material properties are achieved by applying a standard homogenization technique based on unit cells [13]. This numerical homogenization method including the representative volume element (RVE) approach in combination with the FEM was presented in [14] and demonstrated that this method can be used for several kinds of heterogeneous materials, the results also have shown a good agreement with several other homogenization methods.

The PZT sensor is located in parallel (in 0°) to the actuator on both top and bottom layers with a distance of 180 mm. The material properties of the PZT actuator/sensor are presented in [1]. The PZT elements are bonded to the cover plates, cf. Fig. 3. A zero voltage is applied to the bottom surfaces of the sensors and the actuator. The exciting voltage signal of a three and a half-cycle narrow band tone burst (V_{in}) is applied to the top nodes of the actuator [1] (t is time, f_c is central frequency and $H(t)$ is the Heaviside step function).

$$V_{in} = V[H(t) - H(t - 3.5/f_c)]\left(1 - \cos\frac{2\pi f_c t}{3.5}\right)\sin 2\pi f_c t. \quad (1)$$

All nodes on the free surface of the PZT actuator and sensors are tied together to represent the conductivity of the thin copper layer on this area, cf. Fig. 3.

It has been shown in [1,9] that using an element size of less than one tenth of the wave length will result in a good numerical

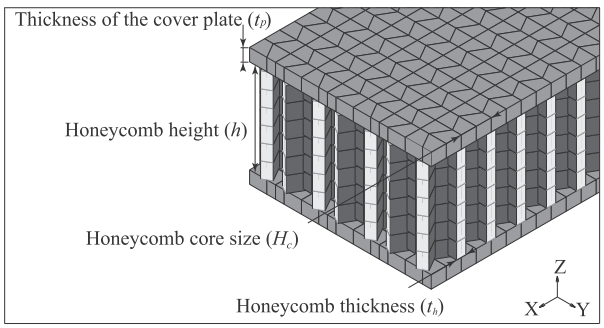

Fig. 2. The sandwich panel design and geometrical properties, also cf. Table 1.

Table 1
The geometrical properties of the sandwich panel and PZT actuator/sensor [1]. These properties will remain constant within this study (units are in mm).

Skin plate		Honeycomb cell	PZT actuator and sensor		
Length	Width	Height	Radius	Thickness	Actuator/sensor distance
290	124	15	3.17	0.7	180

Table 2
Material properties of the plate and the honeycomb cells.

Young's modulus (GPa)		Poisson's ratio (–)		Density (kg m^{-3})	
Skin plate (aluminum alloy T6061 [1])					
70		0.33		2700	
$E_x = E_y$ (GPa)	E_z (GPa)	υ_{xy} (–) and $\upsilon_{yz} = \upsilon_{xz}$ (GPa)	G_{xy} (GPa)	$G_{yz} = G_{xz}$ (kg m^{-3})	Density
Honeycomb cell (HRH-36-1/8-3.0) [1]					
2.46	3.4	0.3	0.94615	1.154	50

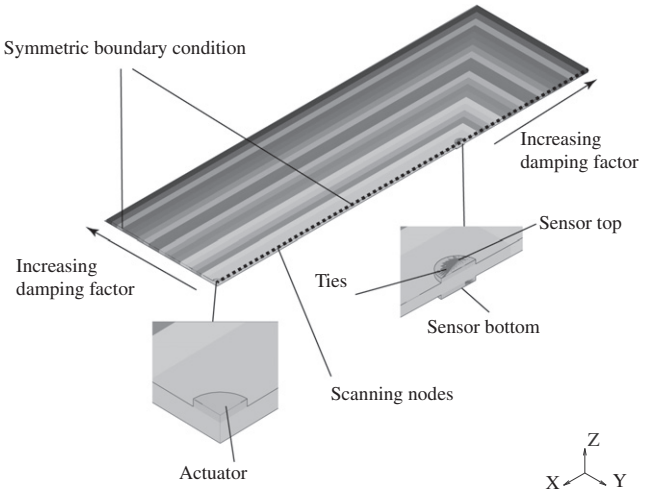

Fig. 3. The orientation of the PZT elements, symmetric boundary condition and non-reflecting boundary condition are shown.

convergence, which also corresponds to the experimental results. In addition, a convergence test is done in the present paper. A loading signal with 200 kHz of the central frequency is applied to generate Lamb waves in an aluminum plate with a thickness of 2 mm. At first element size of one tenth per wave length is considered and then the element size is decreased to one twentieth per wave length. The group velocity of S_0 is calculated in both tests and only 3% difference is observed.

The accuracy of the time integration is also is taken into account [15]. The residual force (F_{res}) for each time step is calculated for a single node from a traction-free surface as follows:

$$M \cdot \ddot{u}_n(t) + K \cdot u_n(t) = F_{res}(t), \tag{2}$$

where M is the mass matrix and K is the stiffness matrix for the surrounding of the considered node and ü is the nodal acceleration and u is the nodal displacement. In a particular example, the residual force is calculated for the maximum time step which is considered in this study. The accuracy of the time integration is indicated as the residual force tends close towards zero and at each time step its maximum magnitude is ten times below the magnitude of the elastic and the inertia forces.

To reduce the model size and the computational costs, symmetric boundary conditions are applied to the inner borders of the plate, cf. Fig. 3, where all the nodes which are on these surfaces cannot move in the direction of the surfaces' normal vectors.

In addition, to reduce the influence of the reflected modes from the outer borders, an exponentially increasing damping boundary is used which was introduced in [16]. The damping factors are increased from the non-damped elements inside the plate to very high damping factors at the outer borders of the plate. The damping factors are highlighted in Fig. 3.

The commercial finite element package ANSYS® 11.0 is used for the simulations.

3. Methodology and signal processing

The Lamb waves propagate along the media with different wave forms, which are known as modes. Each mode can be either a symmetrical (S) mode or an anti-symmetrical (A) mode, cf. Fig. 4. To identify different modes in thin plates one can subtract (or add) the signal on the top and on the bottom surfaces of the plate [17]. However, this method is not suitable for thick sandwich panels where the arrival of the modes on top and bottom surfaces differs. In this paper different modes are identified by using the amplitudes of the arrival signals.

The energy transmission diagrams help to understand the leaky behavior of the propagated waves within a sandwich panel [17]. Comparing the energy transmission rate on the top and bottom surfaces, shows how deep waves can travel inside a sandwich panel. Energy transmission proportion is defined within this paper as the integral over the squared signal [18].

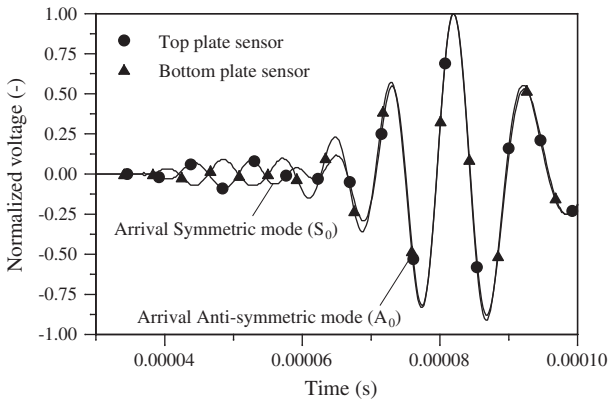

Fig. 4. The arrival symmetrical (S_0) mode and the anti-symmetrical (A_0) mode are plotted in the time domain using a normalized voltage obtained from two sensors on two sides of an isotropic aluminum plate with a plate thickness of 2 mm. The mechanical properties are presented in Table 2. The central frequency of the loading signal is 100 kHz.

$$E_{trans} = \int_{t_{start}}^{t_{end}} V^2(t) \cdot dt. \tag{3}$$

Dispersion curves are used to show the number of waveforms as well as their time of the flight. Two common dispersion curves are the group velocity and the phase velocity. Different modes propagate with different velocities, called group velocity [3]. The phase velocity of a wave is usually associated with the phase difference between the vibrations observed at two different points during the passage of the wave [19]. Using the phase velocity, one can obtain the wave length of each mode. The wave length is an important factor to show the sensitivity of the Lamb waves to detect damages [3].

Within this paper, two different methods are used to evaluate the dispersion curves. In the first method, the so called actuator/sensor method, the received signal from the sensor is compared with the loading signal exited by the actuator in order to achieve the wave properties. In the second approach, the so called scanning method, the scan of the displacements of the nodes between actuator and sensor in direction of the wave propagation are considered to evaluate the wave properties, e.g. experimental data obtained by laser vibrometer measurements. The scanning method has a higher accuracy in comparison to actuator/sensor method while more data are used in this method to examine the wave propagation. However, it is shown later that both methods are corresponding.

3.1. Actuator/sensor method

In this method the received signal from the sensor is examined with the loading signal to evaluate the wave properties. In order to evaluate the group velocity dispersion curves of the propagated waves, the continuous wavelet transform (CWT) based on the Daubechies wavelet D10 is used [2,18], cf. Fig. 5. The time of the flight for each mode corresponds to the time of the maximum value of the CWT coefficients which corresponds to the highest frequency value located in the middle of the propagated mode, cf. Fig. 5. Obtaining the time of flight and knowing the distance between sensor and actuator (180 mm in our case) one can calculate the group velocity for each mode [18]. It must be mentioned here that in this paper the group velocity values calculated using CWT are lower compare to values obtained from the analytical solution. This can be explained by the fact that the flight time is measured by a single sensor PZT and measurement starts from the beginning of the wave excitation by the actuator.

Furthermore, to compute the phase velocity and the wave length of each mode a fast Fourier transform algorithm is used to obtain the phase function as

$$\phi(\omega) = tan^{-1}[\overline{F}_2(\omega)/\overline{F}_1(\omega)], \tag{4}$$

and the phase velocity can be expressed in terms of the frequency as

$$\upsilon(f) = \frac{2\pi f L}{[\phi(f) - \phi_0]}, \tag{5}$$

where f is the frequency, ϕ_0 is the loading phase, $\phi(f)$ is the received phase and L stands for the axial distance between the actuator and the sensor. Clearly, the wave length is calculated by dividing the phase velocity by the loading frequency as

$$\lambda(f) = \frac{\upsilon(f)}{f}. \tag{6}$$

In addition, the group velocity U can then be calculated from the derivatives of the phase spectrum [19] from

$$U(\omega) = L\frac{d\phi}{d\omega}, \tag{7}$$

and in terms of the frequency from

$$U(f) = 2\pi L\frac{d\phi}{df}, \tag{8}$$

and subsequently, the group velocity values obtained with the early described CWT method can be validated comparing to the obtained values from Eq. (8) using the fast Fourier transform algorithm.

3.2. Scanning method

In this method the velocity (displacements) of the nodes perpendicular to the upper side are measured with a scanning laser vibrometer to evaluate the wave properties [20,21]. Fig. 6 shows the setup configuration to examine the Lamb wave propagation in a CFRP plate using scanning laser vibrometer [22].

In a finite element analysis these data correspond to the nodal displacement normal to the plate surface. The results are collected in a so called B-scan diagram, cf. Fig. 7. The B-scan diagram includes the displacements of the nodes (shown in Fig. 3) along the wave propagation direction in the time domain. The ratio of the white solid lines shown in Fig. 7, indicates the phase velocity of each mode [21].

Using the B-scan diagram and applying the second Fourier transformation one can evaluate the dispersion curves, cf. Fig. 8. The first Fourier transformation transforms the results from the time domain to frequency domain and the second Fourier transformation transforms the results from the spacial domain to the wave number domain [20,21]. Using the values in Fig. 8 and Eqs. (5)–(7) the wave propagation properties, such as group velocity and wave length, can be calculated.

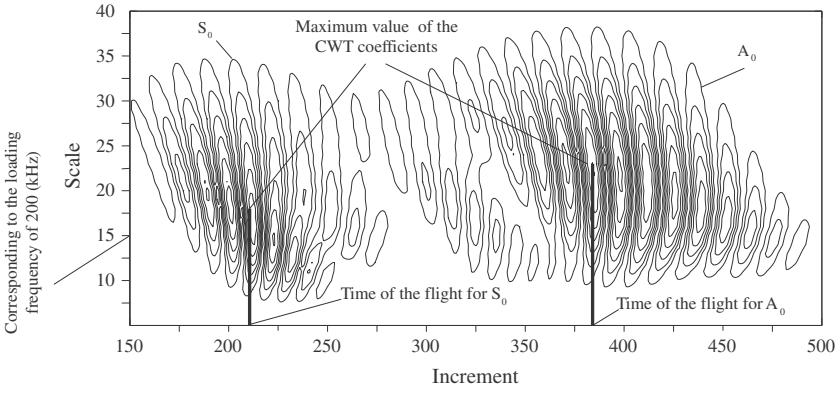

Fig. 5. The contour plot of the absolute values of the CWT coefficients based on the Daubechies wavelet D10 is shown. The signal is obtained from the wave propagation in a honeycomb sandwich panel, cf. Table 2, the central frequency of the loading signal is 200 kHz.

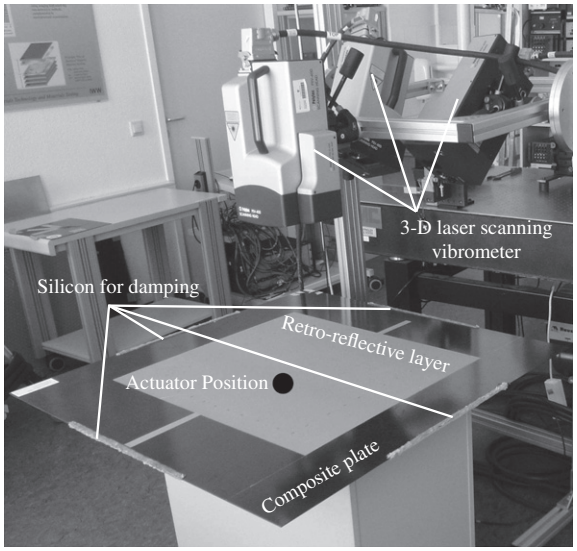

Fig. 6. Setup for experimental test.

The actuator/sensor method is a low-cost method for online health monitoring techniques, therefore in following sections the results will be present based on this technique. However, because of higher accuracy of the results from the scanning method, these results are used to validate the actuator/sensor method approach.

The post-processing calculations are performed with help of MATLAB®.

4. Results

The Lamb wave propagation within a plate is highly depended on

- the loading frequency,
- the geometrical dimensions,
- the material properties [3].

4.1. Lamb wave propagation in honeycomb sandwich plates

4.1.1. Influence of the loading frequency (f_c)

In this part the influence of changes in the central frequency of the loading signal is presented. Wave propagation properties are studied in the frequency range of 40–400 kHz. The chosen loading central frequency is the suitable range for SHM applications for honeycomb sandwich plates while the generated Lamb waves within this range of frequency propagate inside the structure with a reliable wave length for SHM applications. The geometrical properties are constant (t_p is equal to 0.50 mm, t_h is equal to 1.48 mm and H_c is equal to 4.80 mm).

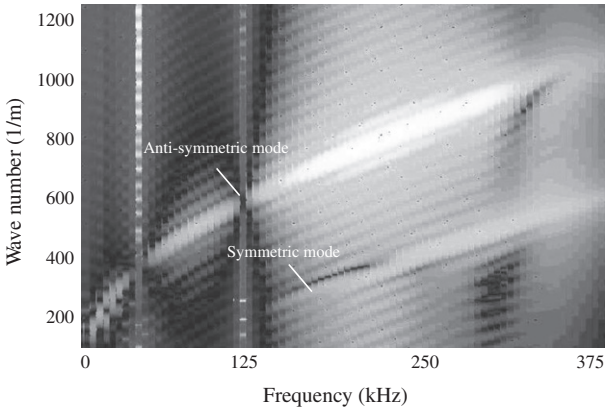

Fig. 8. The results of second Fourier transformation on the B-scan results, which are shown in Fig. 7, plotted over wave number and frequency.

The influence of the changes in the central frequency of the loading signal on the group velocity of the propagated Lamb waves on the top and the bottom surfaces of a honeycomb sandwich plate with the same properties as described earlier in this section, was presented in [25]. It has been reported that the group velocity of the S_0 mode is independent of changes in central loading frequencies in the chosen range of 40–400 kHz. The average group velocity of the S_0 mode on the top surface has been found equal to 4000 m/s while this value decreases to roughly 3400 m/s on the bottom surface. In addition, the group velocity of the A_0 mode has been reported independent of changes in the frequency as the loading central frequency exceeds 150 kHz. In this case the group velocity of the A_0 mode increases from 500 m/s for the central frequency of 40 kHz to the stable value of approximately 2600 m/s for the central frequency of 150 kHz and more. It has been reported that the A_0 mode propagates with nearly the same velocity (with a maximum ±4% difference) on both top and bottom surfaces.

In the present study it is found that the central frequency of the loading signal has a significant influence on the wave length values, cf. Fig. 19. The wave length of the S_0 mode on the top surface decreases from 0.050 mm for the central frequency of 100 kHz to 0.010 mm for the central frequency of 400 kHz. While, the wave length of the A_0 mode on the top surface decreases from

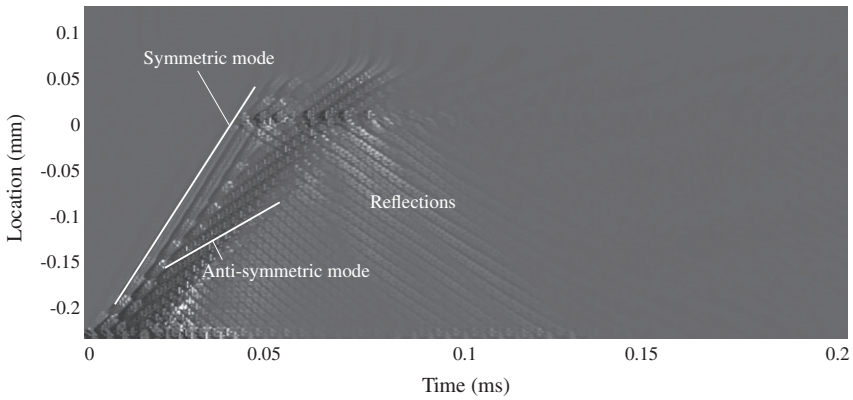

Fig. 7. B-scan diagram of Lamb wave propagation in a honeycomb sandwich plate where t_p is 2 mm, t_h is 0.22 mm, H_c is 4.8 mm, and the rest of geometrical properties are presented in Table 1, the central frequency of the loading signal is 250 kHz.

0.024 mm for the central frequency of 40 kHz to 0.009 mm for the central frequency of 400 kHz. It is found that the wave lengths of the S_0 mode on the bottom surface are 25% lower than on the top surface. But the wave lengths of the A_0 mode on both bottom and top surfaces are nearly the same (with maximum ±5% difference).

Fig. 9 shows the values of the integration of the squared signal in the time domain which represent the energy transmission over the frequency. It is shown that the A_0 mode transmits more energy to the sensor for a certain range of frequency. However, as the frequency exceeds a certain value (the so called critical frequency) the S_0 mode transmits more energy than the A_0 mode to the sensor. In addition, it is clear that the value of the critical frequency is less for the bottom surface in comparison to the top surface.

4.1.2. Influence of the geometrical properties

In this part the influence of the following geometrical properties of the sandwich panel on the wave propagation properties are considered, cf. Fig. 2.

(a) Influence of the cover plate thickness (t_p).
(b) Influence of the honeycomb thickness (t_h).
(c) Influence of the honeycomb core size (H_c).

In all cases the central frequency of the loading signal is 100 kHz. In each case the geometrical properties change in a range of dimensions of available honeycomb sandwich plates in the market.

4.1.2.1. Influence of the cover plate thickness (t_p). In this section the influence of the thickness of the cover plate on the wave propagation is considered, cf. Fig. 2. The cover plate thickness changes from 0.5 mm to 2 mm.

The cover plate thickness does not have a significant influence on the group velocity values. For different cover plate thicknesses, the group velocity of the S_0 mode on the top surface is approximately 4000 m/s and on the bottom surface it is approximately 3400 m/s. The group velocity of the A_0 mode on both top and bottom surfaces is nearly 2000 m/s.

It is found that the thickness of the cover plate does not influence significantly the wave lengths of the propagating Lamb waves in a honeycomb sandwich plate. For different cover plate thicknesses, the wave length of the S_0 mode on the top surface is approximately 0.050 mm, which reduces by 25% on the bottom surface. The wave length of the A_0 mode remains approximately 0.012 mm on both top and bottom surfaces (with maximum difference of ±5% on each surface).

Fig. 10 demonstrates that changes in the thickness of the plate have a minor influence on the energy transmission on the top surface. The energy transmission of the S_0 mode to the bottom surface decreases as the thickness of the cover plate increases. However, the cover plate thickness has less effect on the energy transmission to the bottom surface by the A_0 mode. This phenomenon is also shown in Fig. 18 part (c) and (d) where t_h is constant and equal to 1.48 mm.

4.1.2.2. Influence of the honeycomb thickness (t_h). In this section the influence of the wall thickness of the honeycomb core on the wave propagation is considered, cf. Fig. 2. The honeycomb thickness changes from 0.2 mm to 1.75 mm.

In general, the group velocity is not influenced by the honeycomb wall thickness. For different honeycomb thicknesses, the average group velocity of the S_0 mode on the top surface is 4000 m/s and on the bottom surface it is 3400 m/s. The group velocity of the A_0 mode on both top and bottom surfaces is 2000 m/s.

The results show that the honeycomb wall thickness does not change the wave length significantly. On the top surface, the average wave length of the S_0 mode is 0.050 mm and on the bottom surface these values reduce by 25%. The wave length of the A_0 mode is approximately 0.012 mm both on top and bottom surfaces (with maximum ±5% difference on each surface).

In general, as Fig. 11 shows, changes in the honeycomb wall thickness does not change the energy transmission on the top surface, but on the bottom surface. As the honeycomb wall core increases, the energy transmission increases as well. These results are visualized in Fig. 18 parts (b and d), where t_p is constant and equal to 2.00 mm. However, this phenomenon is more obvious in parts (a and c) where t_p is 0.50 mm. This behavior can be explained by the fact that by increasing the honeycomb wall core thickness the general density of the core layer in the honeycomb sandwich increases and more energy leaks to the bottom plate.

4.1.2.3. Influence of the honeycomb core size (H_c). In this section the influence of the honeycomb core size on the wave propagation is considered, cf. Fig. 2. The honeycomb core size changes from 2.88 mm to 7.2 mm.

It is found that as the honeycomb core size increases the group velocity on the top surface changes subsequently. The group velocity of the S_0 mode increases in a linear shape from 2400 m/s for the honeycomb core size of 2.88 mm to 4000 m/s for the honeycomb core size of 4.8 mm and more. However, on the bottom surface the group velocity of the S_0 mode is less influenced by the honeycomb core size and remains around 3400 m/s for different honeycomb core sizes. The group velocity of the A_0 mode on both

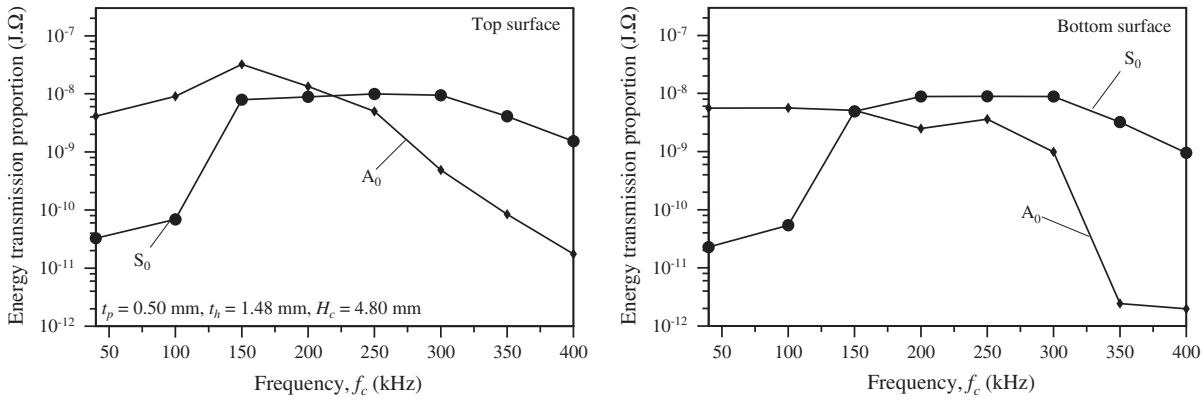

Fig. 9. The energy transmission plotted over the central frequency of the loading signal (f_c), where the geometrical properties are constant, cf. Table 1. The values are plotted using logarithmic scale.

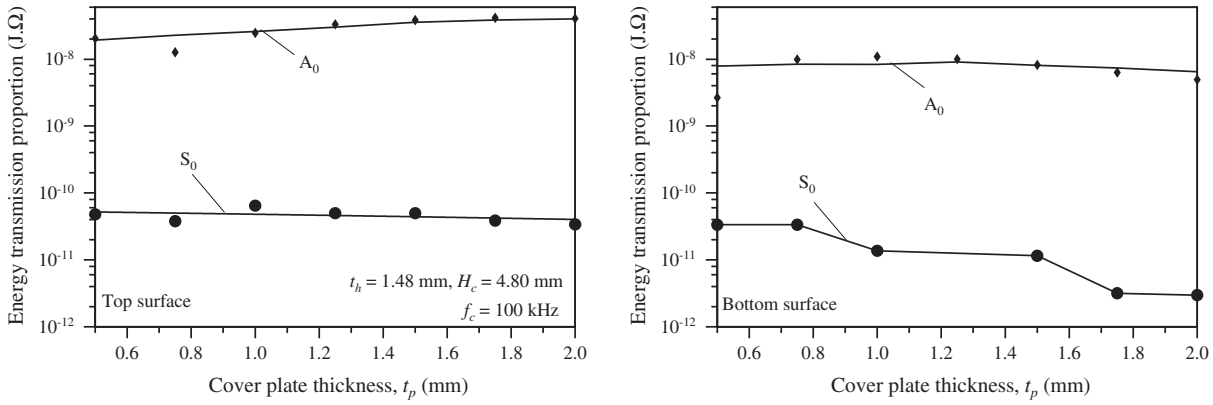

Fig. 10. The energy transmission plotted over the thickness of the cover plate (t_p), where t_h, H_c, and f_c are constant. The values are plotted using logarithmic scale.

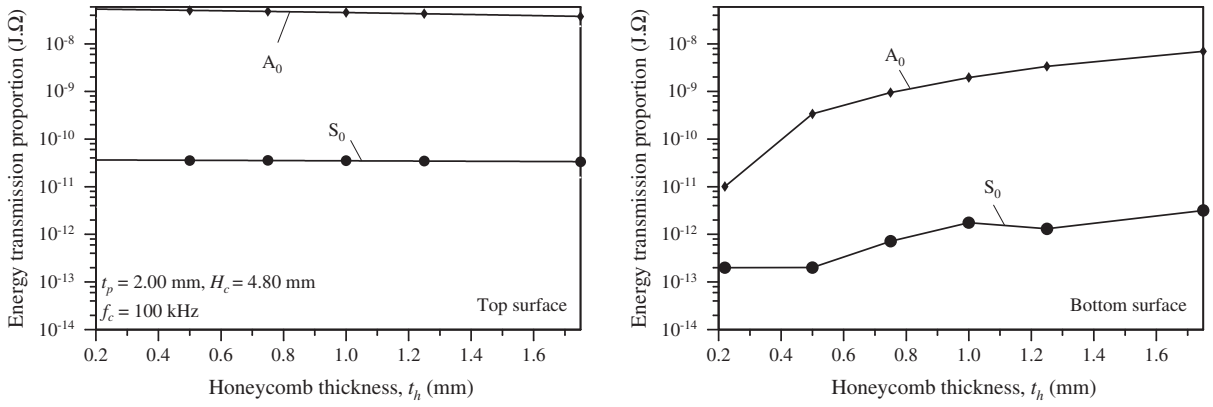

Fig. 11. The energy transmission plotted over the thickness of the honeycomb wall core (t_h), where t_p, H_c, and f_c are constant. The values are plotted using logarithmic scale.

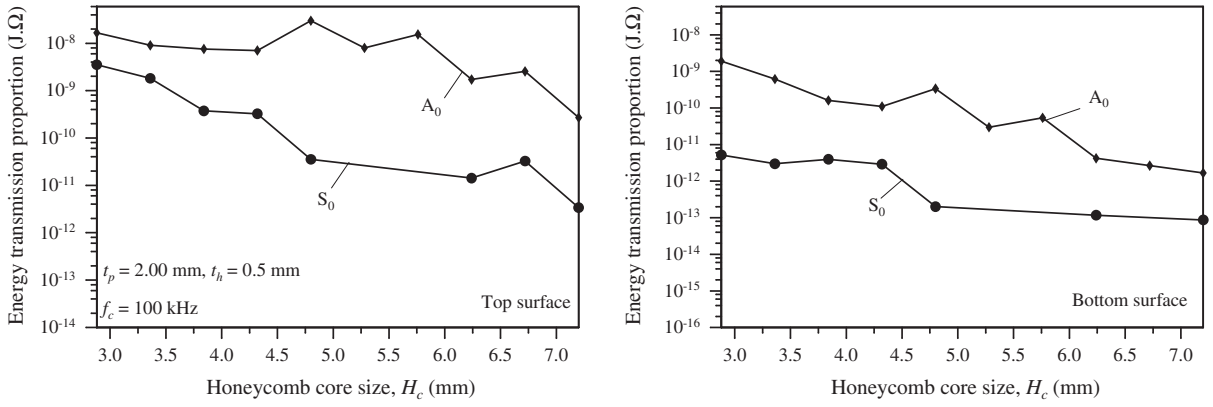

Fig. 12. The energy transmission plotted over the honeycomb core size (H_c), where t_p, t_h, and f_c are constant. The values are plotted using logarithmic scale.

top and bottom surfaces increases in a linear shape from 1400 m/s for the honeycomb core size of 2.88 mm–2000 m/s for the honeycomb core size of 4.8 mm and more.

The wave length of the S_0 mode on the top surface increases in a linear shape from 0.030 mm for the honeycomb core size of 2.88 mm to an average value of 0.050 mm for honeycomb core size of 4.8 mm and more, but on the bottom surface these values reduce by 25%. The wave length of the A_0 mode on both top and bottom surfaces starts from 0.012 mm for the honeycomb core sizes of 2.88 mm to 4.8 mm and increases in a linear shape to approximately 0.025 mm for the honeycomb core size of 5.5 mm and more.

The energy transmission values in the honeycomb model decrease as the honeycomb core size increases, cf. Fig. 12. This can be explained by the fact that as the honeycomb core size increases, so that the general material density of the core layer decreases as well and subsequently less energy leaks to the sensors.

4.2. Homogenization

To simplify the complicated geometry of the honeycomb structure a homogenization technique is used, cf. Section 2. In this section the energy transmission values are used to compare the wave

propagation in the honeycomb sandwich panel with a simplified model. The error percentage is calculated as

$$Error = 100 \cdot \frac{log(E_h) - log(E_s)}{log(E_h)}. \quad (9)$$

E_h represents the energy transmission values which is obtained from the honeycomb model, and E_s shows the energy transmission value which are obtained from the simplified model.

4.2.1. Influence of the loading frequency

It is indicated in Fig. 13 that if the central frequency of the loading signal changes from 40 kHz to 400 kHz the energy transmission values in both simplified and honeycomb models have a similar trend.

4.2.2. Influence of the geometrical properties

A similar trend in the results is observed for the simplified and the honeycomb models when the cover plate thickness (t_p), the honeycomb thickness (t_h) and the honeycomb core size (H_c) are changed, cf. Figs. 14–16.

In addition, the group velocity and the wave length values of the propagated waves in the simplified model and the honeycomb sandwich panel are compared as the central frequency of the loading signal and geometrical properties of the sandwich plate are changed. An average difference of 5% is observed for the group velocity values in the simplified model and the honeycomb sandwich panel model. While, it is found that the wave length values obtained from the simplified model and the honeycomb sandwich panel model are not similar (with an average of 25% difference). Further studies must be done to develop more efficient simplification approach for a better comparison of wave length values.

4.3. Three-dimensional visualization of the results

In this part schematic figures are presented to visualize the wave propagation phenomenon in a honeycomb sandwich panel to receive a better understanding of some of the discussed results in the previous sections. Fig. 17 part (a) shows the Lamb wave propagation within a 3-D honeycomb model and a simplified model where the cover plate is made of aluminum, cf. Table 2. In this case two different geometrical properties are taken into account, first a sandwich plate with $t_p = 2.00$ mm and $t_h = 0.22$ mm is considered, and secondly a sandwich plate with $t_p = 0.50$ mm and $t_h = 1.48$ mm is considered. In both cases H_c is equal to 4.80 mm and the rest of the geometrical properties are presented in Table 1. As it is mentioned in Section 4.1.2, the cover plate thickness and the honeycomb wall thickness have a minor effect on the group velocity. This phenomenon can be seen in Fig. 17 part (a), where the S_0 and A_0 modes of the propagated Lamb wave arrive at a same position in same time (increment) in models with different cover plate thickness and different honeycomb wall thickness. Also, a similar wave propagation behavior is shown for the honeycomb model and the simplified one, in the chosen frequency range.

The interaction of the Lamb waves with the sensors is clearly shown in Fig. 17 part (a). The reflections of the converted S_0 mode visualizes and locates the sensors. This figure clarify the capabilities of the Lamb waves for SHM applications to locate geometrical discontinuities such as gaps or failures in honeycomb sandwich panels.

The influence of the cover plate material properties on the wave propagation is presented in Fig. 17 part (b) in which a honeycomb sandwich plate with an anisotropic cover plate made of T800/924 lamina [23] is considered. The wave propagates faster in x direction which is caused by a stiffer material in this direction.

In Fig. 18 a 3-D representation of the wave propagation in a honeycomb sandwich panel is shown. Different geometrical properties are considered. One can see the influence of the honeycomb wall thickness (t_h) and the thickness of the cover plate (t_p) on both top and bottom surfaces. It is obvious if the honeycomb wall thickness increases the wave amplitude also increases on the bottom surface, cf. parts (a and c) or cf. parts (b and d). However, when the cover plate is thicker the wave mostly propagates on the top surface, cf. parts (a and b) or cf. parts (c and d). These phenomena are also presented in Figs. 10 and 11.

4.4. Comparison of different methods

Fig. 19 presents the wave length values of S_0 and A_0 modes over the frequency, which are evaluated using different methods, cf. Section 3. Part (a) compares the values which are obtained from the scanning process and the values which are calculated using the actuator/sensor method. A good agreement between two methods is obvious.

In order to validate the modeling approach, the results from the finite element simplified model which is used in this study are compared with a semi analytical method, the so called SAFE. This method has the advantage of a very good agreement with analytical solutions and of course the experimental results [24]. The part (b) in Fig. 19 compares the wave length values which are obtained from the dimensional finite element model of a simplified sandwich panel with the results from SAFE [26]. A clear similarity can be observed between the results obtained by both methods.

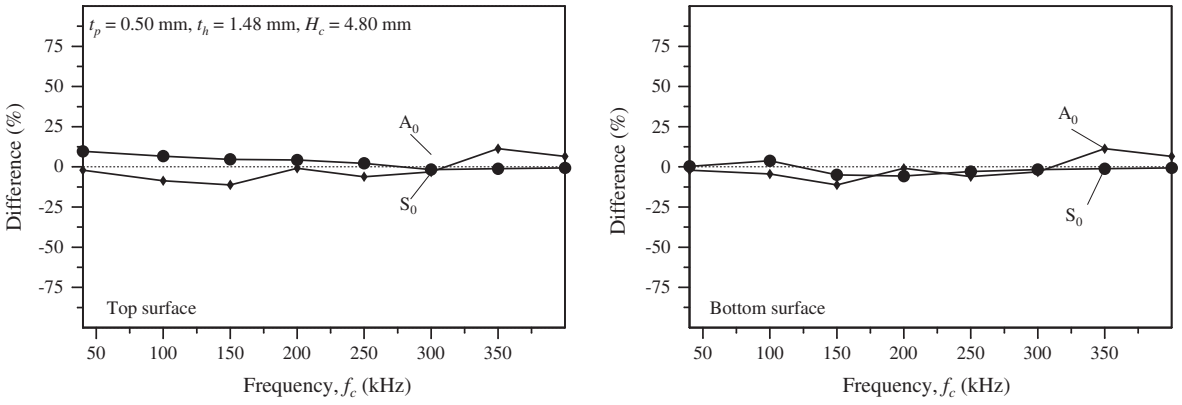

Fig. 13. Error percentage of energy transmission values which are obtained from the simplified model in comparison with the honeycomb model. The values are plotted over the central frequency of loading signal.

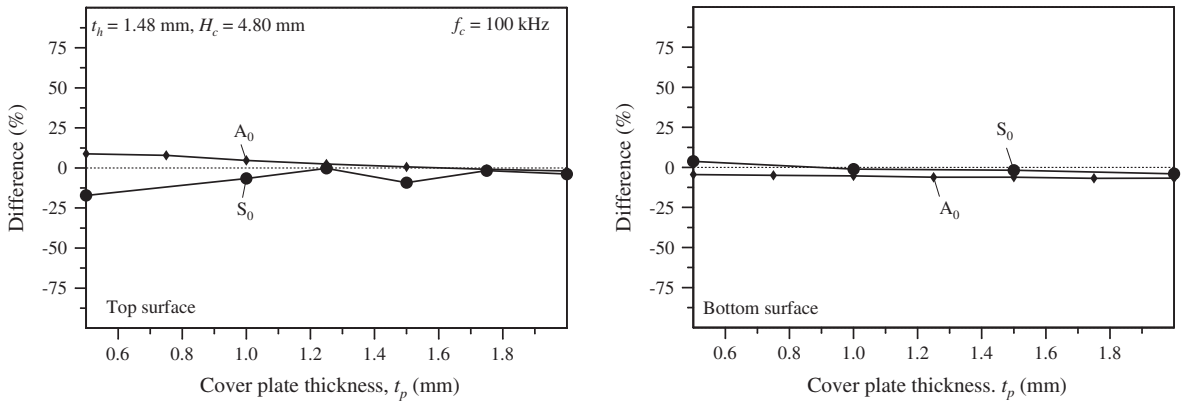

Fig. 14. Error percentage of energy transmission values which are obtained from the simplified model in comparison with the honeycomb model. The values are plotted over the thickness of the cover plate.

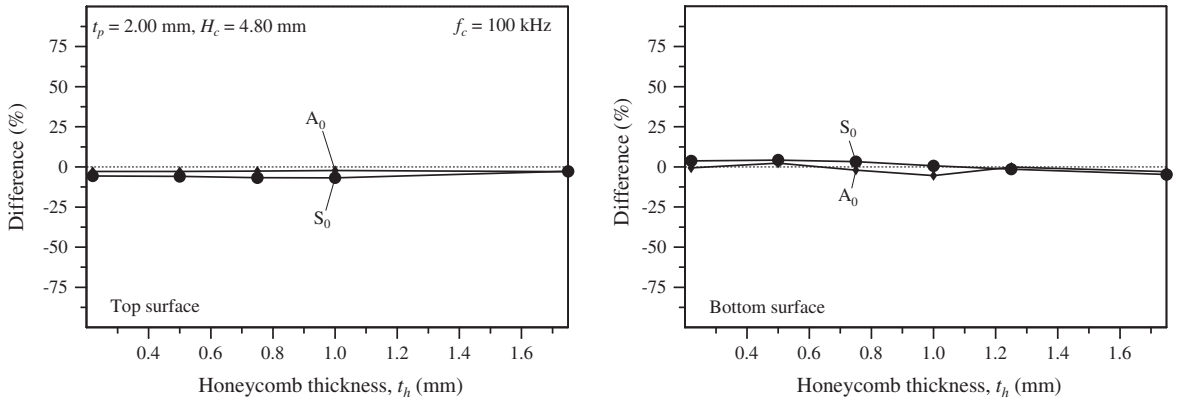

Fig. 15. Error percentage of energy transmission values which are obtained from the simplified model in comparison with the honeycomb model. The values are plotted over the wall thickness of the honeycomb plate.

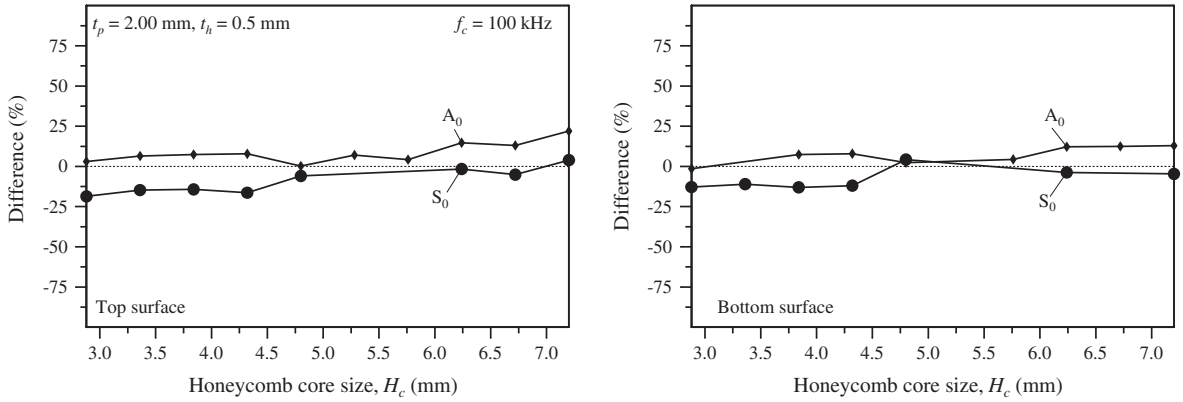

Fig. 16. Error percentage of energy transmission values which are obtained from the simplified model in comparison with the honeycomb model. The values are plotted over the core size of the honeycomb cells.

4.5. Experimental results

In this section the numerical results are compared with the experimental results, cf. Section 3.2 and Fig. 6 for the experimental setup. A honeycomb sandwich panel with a cover plate made of aluminum is considered, cf. Table 2. The honeycomb cell height is 12.7 mm, the cover plate is 0.6 mm thick, the honeycomb cell size is 6.4 mm and the honeycomb wall thickness is 0.635 mm, cf. Fig. 2. Fig. 20 presents the comparison between the group velocities of different modes which are obtained in experimental test and simulation as the central frequency is changed. In addition, the comparison between the wave length of different modes which are obtained in experimental tests and simulations for different central frequencies are presented in Fig. 21. The differences in percentage between the experimental and the numerical values are calculated with Eq. (10) and plotted over the central frequency of the loading signal. V_{exp} stands for the value which is obtained in the experimental test and V_{num} stands for the value which is obtained by the numerical simulation. A clear similarity can be observed.

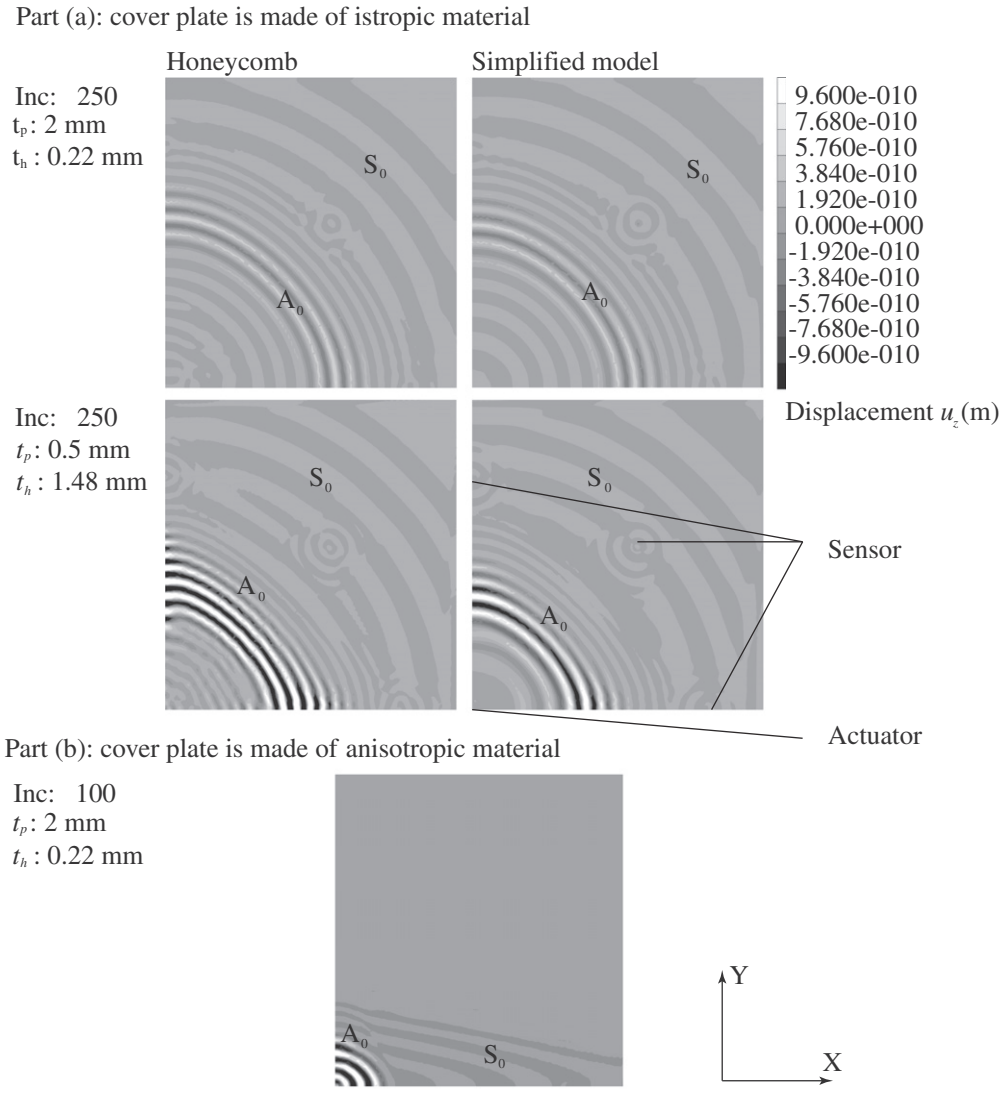

Fig. 17. The wave field of u_z in different sandwich panel structures with different geometrical properties. In part (a) the wave propagation is compared in the honeycomb and the simplified models, the considered cover plate is made of aluminum, cf. Table 2. In part (b) only the honeycomb plate is taken into account and the cover plate is made of anisotropic material of the T800/924 lamina [23]. f_c is 150 kHz and H_c is 4.80 mm.

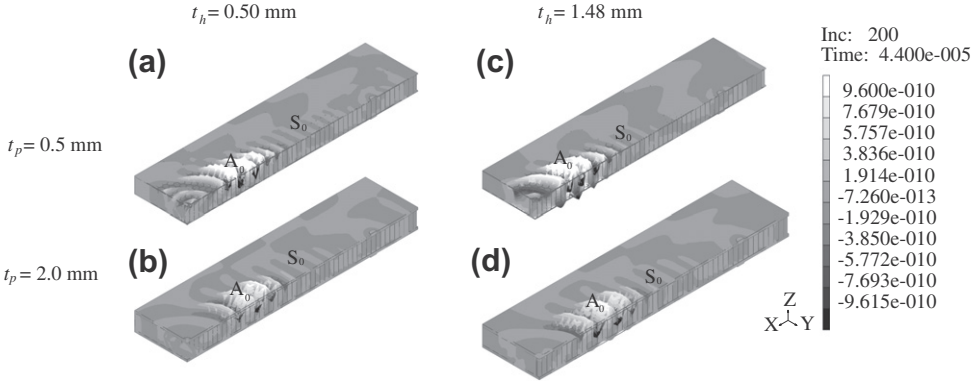

Fig. 18. The wave field of the displacement u_z perpendicular to the plate surface in different sandwich panel structures with different geometrical properties. f_c is 100 kHz and H_c is 4.80 mm.

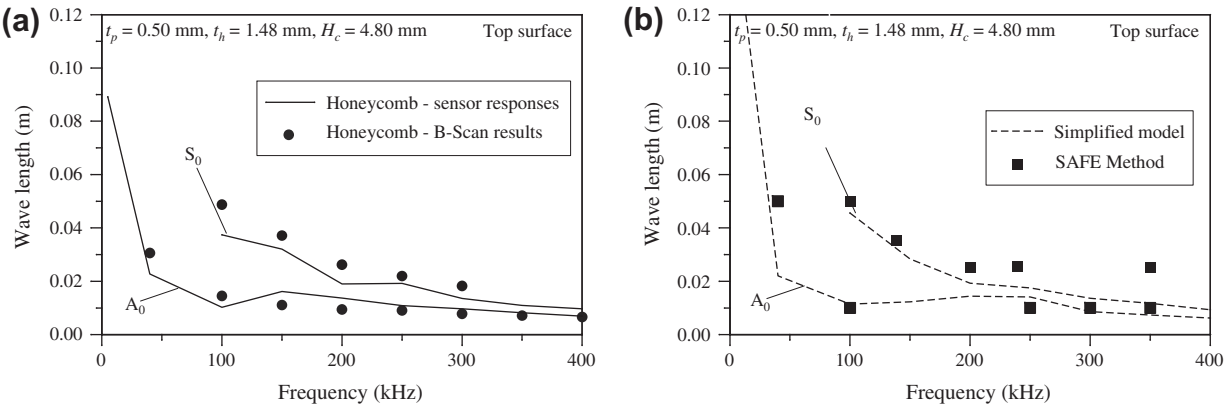

Fig. 19. The wave length values plotted over the frequency, where t_h, t_p and H_c are constant. The values are evaluated by different methods. The part (a) compares the wave length values obtained using the sensor response and the scanning methods, cf. Section 3. The part (b) compares results for the simplified model using a 3-D finite element model (so called simplified model) and the SAFE (semi-analytical method) method [26].

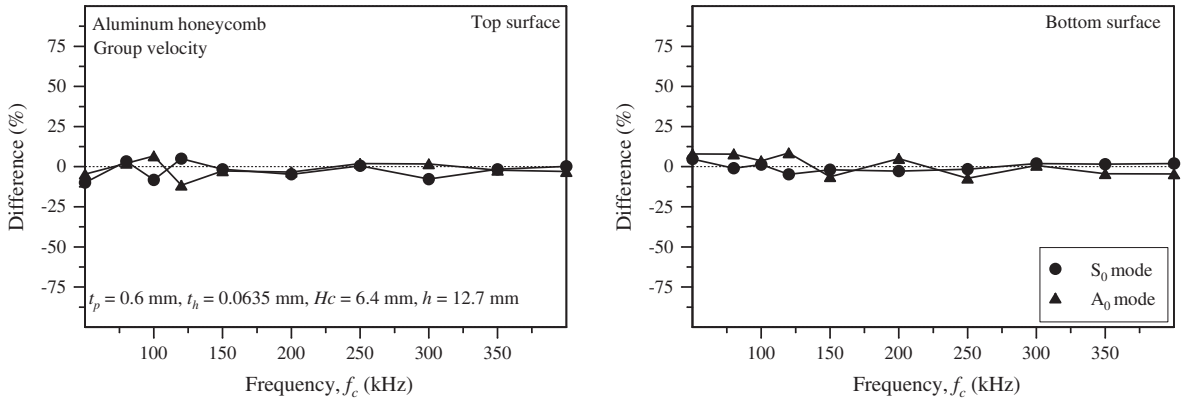

Fig. 20. Comparison of the group velocity values, which are obtained experimentally and numerically. A honeycomb sandwich plate made of aluminum with a height, h, of 12.7 mm, t_p of 0.6 mm, t_h of 0.0635 mm and H_c is 6.4 mm is considered. The central frequency of the loading signal is increased from 50 kHz to 400 kHz.

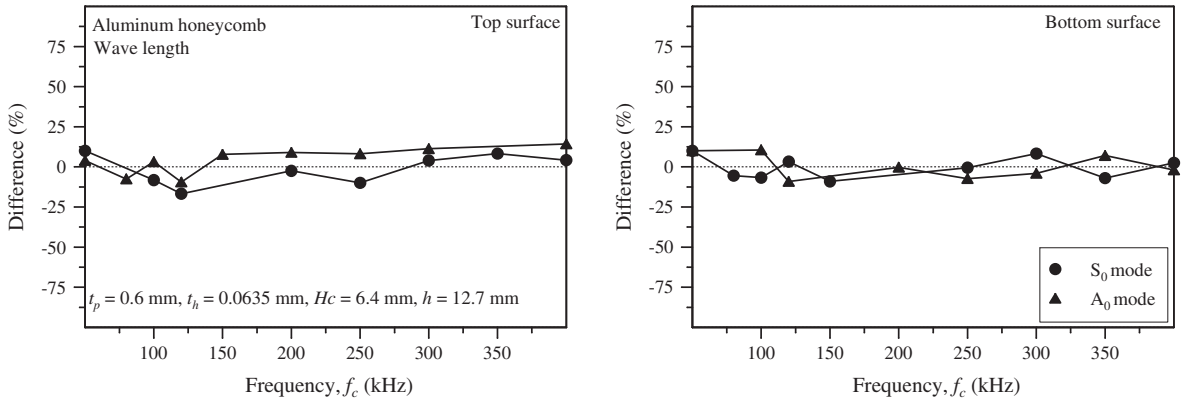

Fig. 21. Comparison of the wave length values, which are obtained experimentally and numerically. A honeycomb sandwich plate made of aluminum with a height, h, of 12.7 mm, t_p of 0.6 mm, t_h of 0.0635 mm and H_c is 6.4 mm is considered. The central frequency of the loading signal is increased from 50 kHz to 400 kHz.

$$Error = 100 \cdot \frac{V_{exp} - V_{num}}{V_{exp}}. \tag{10}$$

4.6. Summary

The wave propagation in honeycomb sandwich panels, which depends on the material properties, the loading frequency and the geometrical dimensions, is studied. To understand the principals of the wave propagation phenomena in honeycomb sandwich panels, a parametric study is performed. To show the influence of each of the properties of the honeycomb sandwich panel on the wave propagation, all parameters are kept constant while only one of them is changed. This parametric study has provided important information to estimate the behavior of the wave in honeycomb sandwich panels. However, it must be mentioned that more investigations are needed to fully describe the wave propagation in any specific honeycomb sandwich panel.

Table 3
The summarizing of the results to show dependency of the wave propagation when the loading frequency and the geometrical dimensions of the honeycomb plate increasing. "↑" indicates an increasing, "–" indicates that there is no change or slight changes and "↓" indicates there is a decreasing in values.

	Group velocity	Wave length	Energy transmission
$f_c \uparrow$	S_0: – A_0: rising to a certain value	↓	Only before critical frequency S_0 is lower than A_0, afterward The S_0 is higher than A_0
$t_p \uparrow$	–	–	S_0 on the top surface: – S_0 on the bottom surface: ↓ A_0: –
$t_h \uparrow$	–	–	Top surface: – Bottom surface: ↑
$H_c \uparrow$	S_0 on the top surface: ↑ S_0 on the bottom surface: – $A_0 \uparrow$	↑	↓

To characterize the wave propagation in honeycomb sandwich plates the group velocity, the wave length and the energy transmission are evaluated. The frequency range of 40–400 kHz and a specific range of geometrical dimensions are considered. In general, it has been reported that the faster S_0 mode has a longer wave length compared to the A_0 mode in the chosen range of frequency and geometry. The parametric study of the wave propagation in models with specific properties shows that for a certain range of frequency the energy transmission rate is higher for the A_0 mode. But as the frequency progresses, the S_0 mode transmits more energy to the sensor.

In general, for the chosen height of the honeycomb sandwich a higher group velocity and a higher wave length for the S_0 mode are received on the top surface compared to the bottom surface (approximately 25% difference). While, for the A_0 mode these data does not differ on both surfaces (approximately 5% difference). However, higher energy transmission rates for both modes on the top surface have been observed compared to the bottom surface (in some cases up to 100% difference). Table 3 summarizes the results, and shows the influence of changes in the geometrical dimensions on the wave propagation in the honeycomb structure.

In addition, a simplified model using homogenization technique is used to simplify the complicated geometry of the honeycomb core structure. The results from the simplified model and the real honeycomb structure are compared and a similar behavior of the waves is observed in both models; however the limitations of using the simplified model are discussed. Also, it has been shown in Fig. 17 that an anisotropic cover plate, results in a non-uniform wave distribution in the structure, where the waves travels faster in the stiffer material direction.

The chosen finite element modeling approach is used in several previous studies, cf. [1,9], and has been validated with experimental results. In addition, within this study, the results are validated and compared with the SAFE method which is a semi-analytical approach. Also, two different approaches including sensor/actuator and scanning methods are used to evaluate the wave properties and similar results have been received from different approaches. Finally, the results are validated experimentally.

5. Outlook

Within this paper the propagation of the Lamb waves within honeycomb sandwich structures is studied. The wave propagation highly depends on the material properties, the loading frequency and the geometrical dimensions of the plate. The wave propagation is characterized by the group velocity, the wave length and the energy transmission. In addition, the results are compared with a simplified model, where the core layer of the sandwich panel is replaced by a homogenized layer. It has been figured out that for a honeycomb structure with specific geometrical properties, the wave propagation properties in the simplified model and the extended 3-D honeycomb model have a similar trend. More investigations are needed to receive more detail information about the wave propagation in honeycomb sandwich plates. However, the parametric study in this paper has provided useful information to show the effects of each of the tested parameters. These information are required for the design of an effective SHM system. Besides numerical studies also experiments are under progress to improve the development of health monitoring systems.

Acknowledgments

By means of this, the authors acknowledge the German Research Foundation for the financial support (GA 480/13); and we would like also to thank C. Willberg for his technical support to carry out the experimental tests.

References

[1] Song F, Huang GL, Hudson k. Guided wave propagation in honeycomb sandwich structures using a piezoelectric actuator/sensor system. Smart Mater Struct 2009;18:125007–15.
[2] Ungethuem A, Lammering R. Impact and damage localization on carbon-fibre-reinforced plastic plates. In: Casciati F, Giordano M, editors. Proceedings 5th European workshop on structural health monitoring. Sorrento, Italy; 2010.
[3] Paget CA. Active health monitoring of aerospace composite structures by embedded piezoceramic transducers. Stockholm, Sweden: Department of Aeronautics Royal Institute of Technology; 2001.
[4] Chang FK, Ihn JB, Blaise E. Design of active structural health monitoring systems for aircraft and spacecraft structures. In: Inman DJ, Farrar CR, Lopes V, Steffen V, editors. Damage prognosis: for aerospace, civil and mechanical systems. John Wiley & Sons Ltd.; 2005. p. 323–41.
[5] Raghavan A, Cesnik CES. Lamb-wave based structural health monitoring. In: Inman DJ, Farrar CR, Lopes V, Steffen V, editors. Damage prognosis: for aerospace, civil and mechanical systems. John Wiley & Sons Ltd.; 2005. p. 235–58.
[6] Thwaites S, Clark NH. Non-destructive testing of honeycomb sandwich structures using elastic waves. J Sound Vib 1995;187(2):253–69.
[7] Wierzbicki E, Woźniak Cz. On the dynamic behavior of honeycomb based composite solids. Acta Mech 2000;141:161–72.
[8] Ruzzene M, Scarpa F, Soranna F. Wave beaming effects in two-dimensional cellular structures. Smart Mater Struct 2003;12:363–72.
[9] Mustapha S, Ye L, Wang D, Lu Y. Assessment of debonding in sandwich CF/EP composite beams using A0 Lamb. Compos Struct 2011;93:483–91.
[10] Qi X, Rose JL, Xu C. Ultrasonic guided wave nondestructive testing for helicopter rotor blades. In: Proceedings 17th world conference on nondestructive testing. Shanghai, China; 2008.
[11] Wang L, Yuan FG. Group velocity and characteristic wave curves of Lamb waves in composites: modeling and experiments. Compos Sci Tech 2007;67:1370–84.
[12] Suranat KS. Transition finite elements for three-dimensional stress analysis. Int J Numer Methods Eng 1980;15:991–1020.
[13] Semkat M. Calculation of the dispersion diagrams for an EC 135 helicopter-tailbooms made of CFRP sandwich panel (in German), Diploma thesis, Institut für Mechanik, Fakultät für Maschinenbau, Otto-von-Guericke-Universität Magdeburg, Germany; 2009.
[14] Kari S. Micromechanical modeling and numerical homogenization of fibre and particle reinforced composites. Düsseldorf: VDI-Verlag; 2007.

[15] Weber R. Numerical simulation of the guided Lamb wave propagation in particle reinforced composites excited by piezoelectric patch actuators, Master thesis, Institut für Mechanik, Fakultät für Maschinenbau, Otto-von-Guericke-Universität Magdeburg, Germany; 2011.
[16] Liu GR, Quek Jerry SS. A non-reflecting boundary for analyzing wave propagation using the finite element method. Finite Elem Anal Des 2003;39:403.
[17] Weber R, Hosseini SMH, Gabbert U. Numerical simulation of the guided Lamb wave propagation in particle reinforced composites. Compos Struct 2012;94(10):3064–71.
[18] Song F, Huang GL, Kim JH, Haran S. On the study of surface wave propagation in concrete structures using a piezoelectric actuator/sensor system. Smart Mater Struct 2008;17:055024–32.
[19] Sachse W, Pao YH. On the determination of phase and group velocities of dispersive waves in solids. J Appl Phys 1978;8:4320–7.
[20] Pohl J, Mook G, Szewieczek A, Hillger W, Schmidt D. Determination of Lamb wave dispersion data for SHM. In: 5th European workshop of structural health monitoring. Italy; 2010.
[21] Köhler B. Dispersion relations in plate structures studied with a scanning laser vibrometer. ECNDT, Berlin; 2006.
[22] Willberg C, Mook G, Gabbert U, Pohl J. The phenomenon of continuous mode conversion of Lamb waves in CFRP plates. Key Eng Mat 2012;518:364–74.
[23] Bartolia I, Marzania A, di Scaleaa FL, Violab E. Modeling wave propagation in damped waveguides of arbitrary cross-section. J Sound Vib 2006;295:685–707.
[24] Vivar-Perez JM, Ahmad ZAB, Gabbert U. Spectral analysis and semi-analytical finite element method for Lamb wave. In: Proceedings of the fifth European structural health monitoring. Naples, Italy; 2010.
[25] Hosseini SMH, Gabbert U. Analysis of guided lamb wave propagation (GW) in honeycomb sandwich panels. PAMM. 2010;1:11–4.
[26] Ahmad ZAB, Gabbert U. Influence of material variations in composite plates on Lamb wave propagation and edge reflection. In: Proceedings of the European conference on computational mechanics. Paris, France; 2010.